

## Photoselective DNA Hairpin Spin Switches

Raanan Carmieli,\* Arun K. Thazhathveetil, Frederick D. Lewis,\* and Michael R. Wasielewski\*

Department of Chemistry and Argonne-Northwestern Solar Energy Research (ANSER) Center, Northwestern University, Evanston, Illinois 60208-3113, United States

**S** Supporting Information

**ABSTRACT:** DNA hairpins having both a tethered anthraquinone (Aq) end-capping group and a perylene-diiimide (PDI) base surrogate were synthesized, wherein Aq and PDI are each separated from a G-C base pair trap by A-T and I-C base pairs (G = guanine, A = adenine, T = thymine, C = cytosine, I = inosine). Selective photoexcitation of PDI at 532 nm generates a singlet radical ion pair (RP),  $^1(\text{G}^+\cdot\text{-PDI}^-\cdot)$ , while selective photoexcitation of Aq at 355 nm generates the corresponding triplet RP,  $^3(\text{G}^+\cdot\text{-Aq}^-\cdot)$ . Subsequent radical pair intersystem crossing within these spin-correlated RPs leads to mixed spin states that exhibit spin-polarized, time-resolved EPR spectra in which the singlet- and triplet-initiated RPs have opposite phases. These results demonstrate that a carefully designed DNA hairpin can serve as a photodriven molecular spin switch based on wavelength-selective formation of the singlet or triplet RP without significant competition from undesired energy transfer processes.

Synthetic DNA hairpins with covalently attached chromophores are versatile systems for investigating photoinduced charge-transfer processes in B-form DNA.<sup>1,2</sup> The relative ease of DNA hairpin synthesis makes them attractive platforms for designing functional molecular materials using light-driven charge transfer. Since excited state charge separation reactions generate radical ion pairs (RPs), it is possible to envision using tailored DNA structures as photon-controlled multispin systems that target organic molecular spintronics and quantum information processing. Time-resolved electron paramagnetic resonance (TREPR) spectroscopy is a powerful tool that can be used to determine spin-selective formation and decay mechanisms of RPs as well as structural information by monitoring their spin dynamics directly on a nanosecond time scale.

We report here an investigation of the DNA hairpins shown in Figure 1 that can function as light-driven molecular spin switches. These hairpins possess a perylene-diiimide (PDI) base surrogate and an anthraquinone (Aq) end-capping group separated by seven base pairs including a single G-C base pair halfway between PDI and Aq, which serves as a hole trap. Excitation of PDI at 532 nm selectively generates the singlet radical ion pair (RP),  $^1(\text{G}^+\cdot\text{-PDI}^-\cdot)$ , whereas excitation of Aq at 355 nm selectively produces the corresponding triplet RP,  $^3(\text{G}^+\cdot\text{-Aq}^-\cdot)$ . Replacement of one A-T base pair with an I-C base pair serves to attenuate the hole transport efficiency between G and either PDI or Aq, thus modulating the intensity

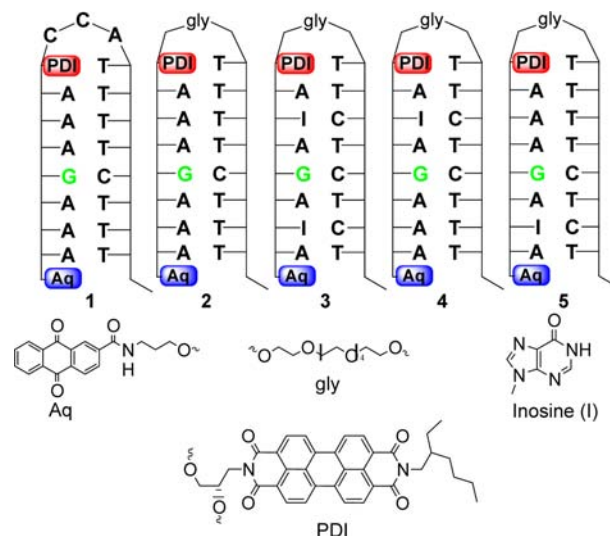


Figure 1. DNA hairpin structures used in this study.

of the TREPR signal. The RPs produced by charge separation in these DNA hairpins exhibit non-Boltzmann spin populations that differ significantly based on whether the initial excited state is  $^1*\text{PDI}$  or  $^3*\text{Aq}$ , thus, providing the basis for a fast, light-driven DNA-based spintronic device.

Previous studies using  $^1*\text{PDI}$  and  $^3*\text{Aq}$  photo-oxidants showed that the RP quantum yield at 85 K is maximal, when the G hole trap is positioned at the fourth base pair position away from the photo-oxidant.<sup>3,4</sup> As a consequence, hairpins 1–5 (Figure 1) were designed with G in the fourth position with respect to both Aq and PDI. This also places Aq and PDI eight base pairs apart, which should be far enough to prevent competitive triplet energy transfer from  $^3*\text{Aq}$  to PDI. We synthesized hairpin 2–5 with a glycol hairpin linker instead of CCA bases in order to prevent any base oxidation in the wrong direction. Hairpins 3–5 were synthesized with inosine incorporated in position 2 relative to Aq and/or PDI. Inosine has an oxidation potential  $E_{\text{OX}} = 1.52$  V which is higher than A,  $E_{\text{OX}} = 1.4$  V, and is therefore used to inhibit charge transfer from G to the photo-oxidant, and thus serves as a tool for controlling charge transfer in a preferred direction.<sup>5</sup> The steady-state UV-vis absorption spectrum of hairpin 1 (Figure 2) shows that PDI absorbs in the region of 450–560 nm and Aq absorbs in the region of 250–400 nm, which permits selective photoexcitation of either chromophore.

Received: June 3, 2013

Published: July 15, 2013

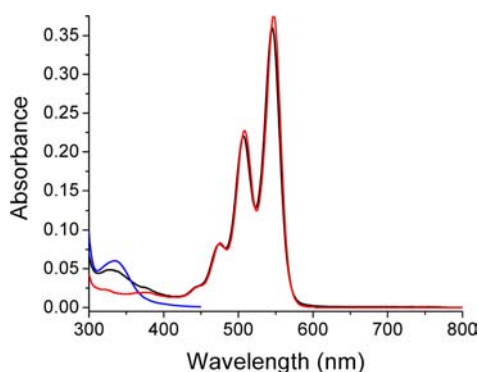


**Figure 2.** Steady-state UV-vis absorption spectrum of **1**, black trace. Aq absorbs up to 400 nm (superimposed blue trace), and PDI absorption range is from 450 to 560 nm (superimposed red trace).

Photoexcitation of donor-acceptor molecules can produce well-defined initial spin states. For example, spin-selective intersystem crossing following photoexcitation often produces highly spin-polarized triplet states.<sup>6</sup> In addition, photoinitiated electron transfer within covalently linked organic donor-acceptor molecules having specific donor-acceptor distances and orientations can result in the formation of highly spin-polarized RPs in which the initial spin state is well-defined.<sup>7,8</sup> In the case of singlet-initiated spin-correlated RPs, photoexcitation of the acceptor in a donor-bridge-acceptor (D-B-A) system to its lowest excited singlet state, D-B-<sup>1</sup>\*A, is immediately followed by rapid, nonadiabatic charge separation to produce the singlet RP, <sup>1</sup>(D<sup>+</sup>•-B-A<sup>-</sup>•). This RP may undergo electron-nuclear hyperfine coupling-induced radical pair intersystem crossing (RP-ISC) in a few nanoseconds to produce the triplet RP, <sup>3</sup>(D<sup>+</sup>•-B-A<sup>-</sup>•). The subsequent charge recombination process is spin selective; i.e., <sup>1</sup>(D<sup>+</sup>•-B-A<sup>-</sup>•) recombines to the singlet ground state D-B-A, while <sup>3</sup>(D<sup>+</sup>•-B-A<sup>-</sup>•) recombines to yield the neutral local triplet <sup>3</sup>\*(D-B-A), (Figure 3a).<sup>9-11</sup> In the presence of a high magnetic field, RP-ISC results in S-T<sub>0</sub> mixing to produce a coherent superposition state (Figure 3b). Since the mixed |S'⟩ and |T'⟩ states both have triplet character,

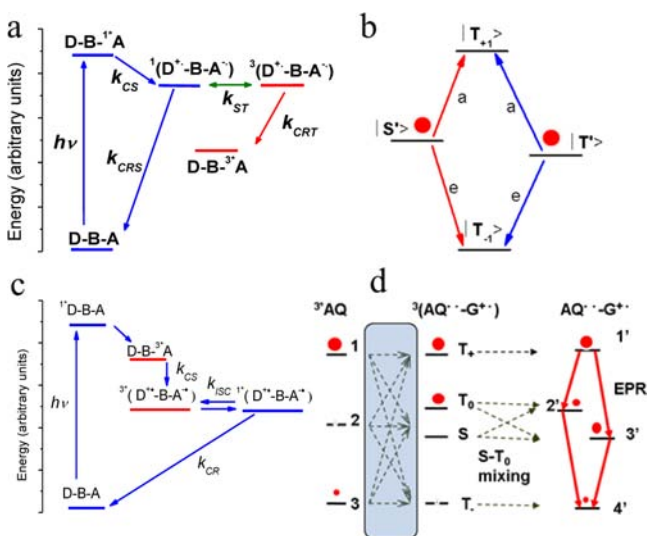


**Figure 3.** (a) Photogeneration of singlet-initiated RPs; (b) RP energy levels following S-T<sub>0</sub> mixing; (c) photogeneration of triplet-initiated RPs; (d) RP energy levels following charge separation from the triplet state.

microwave-induced transitions between these states and |T<sub>+1</sub>⟩ and |T<sub>-1</sub>⟩ result in a spin-polarized EPR spectrum with four equal intensity lines having a symmetric (*e,a,e,a*) anti-phase pattern (where *e* denotes emission and *a* denotes enhanced absorption, low to high field), given that the spin-spin exchange interaction ( $2J$ ) between the two radicals is positive and larger than the dipolar interaction ( $d$ ) between the two spins. If the *g*-factors of the two radicals are similar and/or are split by hyperfine couplings, the two doublets will overlap strongly and will often appear as a somewhat distorted (*e,a*) signal.<sup>12,13</sup>

In contrast, if photoexcitation of a donor-bridge-acceptor (D-B-A) system to its lowest excited singlet, D-B-<sup>1</sup>\*A, is immediately followed by rapid spin-orbit system crossing (SO-ISC) to give D-B-<sup>3</sup>\*A (Figure 3c), the rates of SO-ISC to each of the three spin sublevels of X, Y, and Z in D-B-<sup>3</sup>\*A are generally different.<sup>14</sup> The spin-spin dipolar interaction results in zero-field splitting of the triplet sublevels, which depends strongly on the direction of the magnetic field ( $B_0$ ) with respect to the principal axes (X, Y, and Z) of the molecular triplet axis system.<sup>14</sup> Transfer of electron spin polarization from the D-B-<sup>3</sup>\*A precursor state to the spin states of the RP takes place during the charge separation (CS) reaction if spin-lattice relaxation of the polarized D-B-<sup>3</sup>\*A state is slower than the CS reaction.<sup>15,16</sup> Unlike the singlet-initiated case where the absolute intensities of the transitions are equal due to the equal initial populations of the mixed |S'⟩ and |T'⟩ sublevels, in the case of a spin-correlated RP originating from D-B-<sup>3</sup>\*A, the intensities depend on the initial population of the triplet sublevels (Figure 3d), and as a result the intensities of the four EPR transitions are not necessarily equal, so that the TREPR spectrum can be asymmetric. Because of this difference, it may be possible to encode quantum information in the population differences of these sublevels. For example, we have recently shown that the magnitude of spin polarization transfer from a photogenerated spin-correlated RP attached to a stable radical can be controlled by varying  $2J$  within the RP.<sup>17</sup>

Figure 4a shows the TREPR spectrum following selective photoexcitation of PDI in hairpin **1** with a 532 nm, 7 ns laser

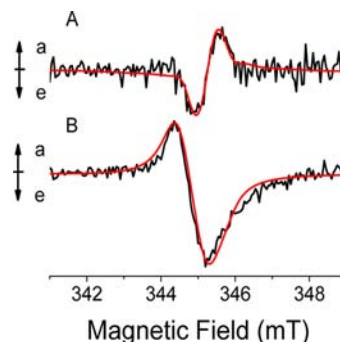


**Figure 4.** TREPR spectra of **1** at 100 ns following a (A) 532 nm laser pulse and (B) 355 nm laser pulse. The superimposed red traces are simulations of the spectra.

pulse. This spectrum is characterized by a symmetric (*e,a*) phase pattern, which results from S-T<sub>0</sub> mixing (Figure 3b). Only the mixed |S'⟩ and |T'⟩ states are initially populated, which upon microwave irradiation produce a symmetric derivative-like (anti-phase) spectrum as described above. Figure 4b shows the TREPR spectrum following selective photoexcitation of Aq in hairpin **1** with 355 nm, 7 ns laser pulse. This

spectrum is characterized by an asymmetric (*a,e*) phase pattern. This results from initial overpopulation of the  $T_{+1}$  sublevel of  $^3(G^{+\bullet}-Aq^{-\bullet})$ , which produces larger emission upon microwave irradiation. The spin-polarized EPR spectra were simulated with home-written MATLAB<sup>18</sup> programs using published models<sup>15,19</sup> and the parameters are summarized in Table 1.

**Table 1. Simulation Parameters for the RP Spectra of 1 Measured by TREPR at 85 K and 100 ns after the Laser Pulse**

excitation (nm)	<i>D</i> (mT)	<i>2J</i> (mT)	<i>r</i> (Å)
532	$-0.9 \pm 0.1$	$0.08 \pm 0.02$	$14.6 \pm 0.5$
355	$-0.9 \pm 0.1$	$0.02 \pm 0.02$	$14.6 \pm 0.5$

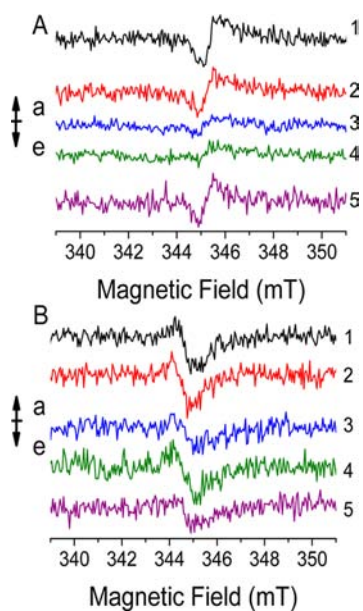


**Figure 5.** TREPR spectra of 1–5 recorded at 85 K 100 ns after a (A) 532 nm laser pulse and (B) 355 nm laser pulse.

Figure 5 shows the TREPR spectra of hairpins 2–5 following photoexcitation at 532 nm (Figure 5a) and 355 nm (Figure 5b) where the spectrum of hairpin 1 serves as a reference. From Figure 5a, it can be seen that using glycol as a hairpin linker instead of CCA does not improve the charge separation efficiency and the signal-to-noise of the spectrum is similar to that of 1 recorded under the same experimental conditions. Hairpins 3–5 have inosine incorporated into the base pair sequence between the photo-oxidants and the G hole trap. The data in Figure 5 show that the intensities of the spin-polarized TREPR spectra of the hairpins having inosine are decreased relative to those without inosine. As noted above, inosine is 0.12 V harder to oxidize than is adenine, so that  $\Delta G$  for the charge separation reactions  $I^{+\bullet}\text{-PDI} \rightarrow I^{+\bullet}\text{-PDI}^{\bullet-}$  and  $I^{+\bullet}\text{-Aq} \rightarrow I^{+\bullet}\text{-Aq}^{\bullet-}$  are both 0.12 V more positive than are the corresponding reactions for adenine, making the photo-oxidation of inosine slower than that of adenine. This most likely results in a more favorable kinetic competition between the  $I^{+\bullet}\text{-PDI}^{\bullet-} \rightarrow I\text{-PDI}$  and  $I^{+\bullet}\text{-Aq}^{\bullet-} \rightarrow I\text{-Aq}$  charge recombination reactions and the corresponding hole transfers from  $I^{+\bullet}$  to G relative to the same comparisons when  $A^{+\bullet}$  is the intermediate hole donor to G. Thus, the substitution of A by I reduces the hole transfer efficiency to G, but it does not block it completely.

These results demonstrate the ability of DNA hairpins to serve as a platform for constructing a wavelength-dependent molecular spin switch that may prove useful for manipulating quantum information using the spin dynamics of photo-generated RPs.

## ■ ASSOCIATED CONTENT

### 📄 Supporting Information

Experimental details including synthesis, mass spectral data, thermal dissociation data, and circular dichroism spectra for 1–5. This material is available free of charge via the Internet at <http://pubs.acs.org>.

## ■ AUTHOR INFORMATION

### Corresponding Author

[m-wasielewski@northwestern.edu](mailto:m-wasielewski@northwestern.edu); [r-carmielli@northwestern.edu](mailto:r-carmielli@northwestern.edu); [fdl@northwestern.edu](mailto:fdl@northwestern.edu)

### Notes

The authors declare no competing financial interest.

## ■ ACKNOWLEDGMENTS

This research was funded by the Office of Naval Research MURI grant no. N00014-11-1-0729. R.C. (EPR) was supported as part of the ANSER Center, an Energy Frontier Research Center funded by the U.S. Department of Energy (DOE), Office of Science, Office of Basic Energy Sciences, under award number DE-SC0001059. The authors thank Dr. P. P. Neelakandan for the PDI-monoDMT derivative.

## ■ REFERENCES

- (1) Lewis, F. D.; Wu, T.; Zhang, Y.; Letsinger, R. L.; Greenfield, S. R.; Wasielewski, M. R. *Science* **1997**, *277*, 673.
- (2) Lewis, F. D.; Liu, X.; Liu, J.; Miller, S. E.; Hayes, R. T.; Wasielewski, M. R. *Nature* **2000**, *406*, 51.
- (3) Zeidan, T. A.; Carmieli, R.; Kelley, R. F.; Wilson, T. M.; Lewis, F. D.; Wasielewski, M. R. *J. Am. Chem. Soc.* **2008**, *130*, 13945.
- (4) Carmieli, R.; Smeigh, A. L.; Mickley Conron, S. M.; Thazhathveetil, A. K.; Fuki, M.; Kobori, Y.; Lewis, F. D.; Wasielewski, M. R. *J. Am. Chem. Soc.* **2012**, *134*, 11251.
- (5) Kelley, S. O.; Jackson, N. M.; Hill, M. G.; Barton, J. K. *Angew. Chem., Int. Ed.* **1999**, *38*, 941.
- (6) Levanon, H.; Norris, J. R. *Chem. Rev.* **1978**, *78*, 185.
- (7) Shaakov, S.; Galili, T.; Stavitski, E.; Levanon, H.; Lukas, A.; Wasielewski, M. R. *J. Am. Chem. Soc.* **2003**, *125*, 6563.
- (8) Hasharoni, K.; Levanon, H.; Greenfield, S. R.; Gosztola, D. J.; Svec, W. A.; Wasielewski, M. R. *J. Am. Chem. Soc.* **1995**, *117*, 8055.
- (9) Steiner, U. E.; Ulrich, T. *Chem. Rev.* **1989**, *89*, 51.
- (10) Weiss, E. A.; Ratner, M. A.; Wasielewski, M. R. *J. Phys. Chem. A* **2003**, *107*, 3639.
- (11) Weiss, E. A.; Ahrens, M. J.; Sinks, L. E.; Gusev, A. V.; Ratner, M. A.; Wasielewski, M. R. *J. Am. Chem. Soc.* **2004**, *126*, 5577.
- (12) Closs, G. L.; Forbes, M. D. E.; Norris, J. R. *J. Phys. Chem.* **1987**, *91*, 3592.
- (13) Buckley, C. D.; Hunter, D. A.; Hore, P. J.; McLauchlan, K. A. *Chem. Phys. Lett.* **1987**, *135*, 307.
- (14) McGlynn, S. P.; Azumi, T.; Kinoshita, M. *Molecular Spectroscopy of the Triplet State (Prentice-Hall International Series in Chemistry)*; Prentice-Hall: Englewood Cliffs, NJ, 1969.
- (15) Kobori, Y.; Shibano, Y.; Endo, T.; Tsuji, H.; Murai, H.; Tamao, K. *J. Am. Chem. Soc.* **2009**, *131*, 1624.
- (16) Akiyama, K.; Tero-Kubota, S. *Mol. Phys.* **1994**, *83*, 1091.
- (17) Colvin, M. T.; Carmieli, R.; Miura, T.; Richert, S.; Gardner, D. M.; Smeigh, A. L.; Dyar, S. M.; Conron, S. M.; Ratner, M. A.; Wasielewski, M. R. *J. Phys. Chem. A* **2013**, *117*, 5314.
- (18) MATLAB; The MathWorks, Inc.: Natick, MA, 2013.

(19) Till, U.; Hore, P. J. *Mol. Phys.* **1997**, *90*, 289.